Desalination and Water Treatment
www.deswater.com
3 (2009) 261–270
1944-3994/1944-3986

Study of a water desalination unit using solar energy

Khalifa Zhani[a], Habib Ben Bacha[b]*, Tarek Damak[c]

[a]*Laboratoire des Systèmes Electro-Mécaniques (LASEM), National Engineering School of Sfax, Sfax University, Tunisia*
[b]*College of Engineering in Alkharj, King Saud University, BP 655-11946, Kingdom of Saudi Arabia*
Tel. +966 506 678 408; Fax: +966 1 553 964; email: hbacha@ksu.edu.sa
[c]*Unité de commande des Procédés Industriels, National Engineering School of Sfax, Sfax University, Tunisia*

Received 31 August 2008; Accepted 2 February 2009

ABSTRACT

This paper presents the study of a water desalination new design process working with the humidification–dehumidification (HD) method using solar energy. This process was developed in order to boost the productivity of the solar multiple condensation evaporation cycle unit which is located at the national school of engineering of Sfax, Tunisia, by integrating into the latter a flat-plate solar air collector and a humidifier. The HD process is essentially composed of a flat-plate solar air collector, a flat-plate solar water collector, a humidifier, an evaporation tower and a condensation tower. A general model based on heat and mass transfers in each component of the unit has been developed in a steady-state regime. The obtained set of ordinary differential equations has been converted to a set of algebraic system of equations by the functional approximation method of orthogonal collocation. The developed model is used to simulate the HD system in order to investigate the steady-state behavior of each component of the unit and the entire system exposed to a variation of the entrance parameters and meteorological conditions.

Keywords: Solar energy; Water desalination; Humidification–dehumidification; Modeling; Simulation

1. Introduction

Tunisia, like many other countries in the world, is confronted with three main problems [1,2]: fresh water scarcity, fossil energy depletion and environmental degradation due to gas emissions. Unlike the fossil energy situation, Tunisia has an abundance of renewable energies, especially solar energy. So, desalination by means of renewable energy sources is a suitable solution for providing fresh water for some remote regions in Tunisia and in other countries.

The majority of conventional desalination techniques such as multi-stage flash (MSF), multi-effect (ME), vapor compression (VC) and reverse osmosis (RO) are only reliable for large capacity ranges of 100–50,000 m^3/day of fresh water production [3]. These technologies are costly for small amounts of fresh water, inefficient from the viewpoint of energy consumption and require high maintenance due to the practical difficulties associated with the high operating temperature, like corrosion and scale formation. Moreover, the use of conventional energy sources to drive these technologies has a negative impact on the environment. However, solar energy is free, abundant and an environmentally friendly energy source. Combining the principle of humidification–dehumidi-

*Corresponding author.

Presented at EuroMed 2008, Desalination for Clean Water and Energy Cooperation among Mediterranean Countries of Europe and the MENA Region, 9–13 November 2008, King Hussein Bin Talal Convention Center, Dead Sea, Jordan.

fication (HD) with solar desalination leads to an increase on the overall efficiency of the desalination system and therefore appears to be the best method of water desalination with solar energy [4].

The major inconvenience of a solar desalination unit based on the HD principle is its limited production of fresh water. Thus, according a review of the literature, there are many investigators who have developed and studied various solar desalination systems using the HD principle. These studies discussed ways to boost fresh water production.

In 2007, a theoretical study of a solar desalination with humidification–dehumidification (SDHD) process at Monastir, Tunisia, was conducted by Orfi et al. [5]. The SDHD unit includes air and water solar collectors and a separate evaporator and condenser. They conducted various simulations, showing the effects of the relevant non-dimensional parameters on the daily and yearly fresh water production.

In 2006, Al-Enezi et al. [6] measured and analyzed at low operating temperatures the performance characteristics of a HD desalination system which included a packed humidification column, a double pipe glass condenser, a constant temperature water circulation tank and a chiller for cooling water. Water production is found to depend strongly on the hot water temperature. Also, water production is found to increase upon the increase of the air flow rate and the decrease of the cooling water temperature.

In 2004, Nafey et al. [7] presented a numerical investigation of humidification–dehumidification desalination (HDD) principle using solar energy. The HDD system consists mainly of a concentrating a solar water heating collector, flat-plate solar air heating collector, humidifying tower and dehumidifying exchanger. The obtained results show that the system productivity was strongly affected by the solar intensity, air flow rate and cooling water flow rate. The ambient temperature has an insignificant effect on the system productivity. The numerical model used in simulation was evaluated experimentally and with other published works.

In 1999, Ben Bacha et al. [8] studied a new generation of water desalination installation by solar energy using the solar multiple condensation evaporation cycle (SMCEC). principle. The SMCEC-based desalination unit consists of three main parts: water solar collector, condensation tower and evaporation tower. Based on model simulation and experimental validation, the optimum operation and production for this type of system need a perfect insulation of the unit, a high water temperature and flow rate at the entrance of the condenser, hot water recycling by injection at the top of the evaporation chamber and a storage tank to store the hot water excess that would extend water desalination beyond sunset.

As far as we are concerned, to ameliorate the production of solar desalination units based on the HD principle, especially the SMCEC unit, we have added to the latter a flat-plate solar air collector and a humidifier. The present work deals with a theoretical study of the water desalination unit by solar energy using the HD principle. Its underlying objectives are:

- to develop a steady-state mathematical model of the different components of the unit (air and water solar collector, humidifier, evaporation tower and condensation tower), and
- to study the behavior of key output parameters for each component of the unit.

2. System description

Figs. 1 and 2 present respectively a schematic and a synoptic diagram of the HD process. The solar desalination system under study differs from the previously explored published works by using a humidifier and an evaporation tower, on the one hand, and a field of flat-plate air solar collectors and a field of flat-plate water solar collectors on the other, which makes the system more flexible and increases the fresh water production. Sea or brackish water which is preheated in the condensation tower, by the latent heat of condensation, and heated in the water solar collectors is pulverized into the humidifier and the evaporation tower. Due to heat and mass transfers between the hot water and the heated air stream in the humidifier in case of working in closed air loop and between the hot water and the ambient air stream in the evaporation tower in case of working in open air loop, the latter is loaded by moisture. To increase the surface of contact between air and water, and therefore to raise the rate of air humidification, a packed bed is implanted in the tower of evaporation and the humidifier. The saturated moist air is then transported toward the condensation tower where it comes in contact with a surface, the temperature of which is lower than the dew point of the moist air. The condensed water was collected from the bottom of the condensation tower, while the brine (the salty water exiting the evaporator and the humidifier) at the bottom of both the humidifier and evaporation tower will be either recycled and combined with the feed solution at the entry point or rejected in case of increase of saline rates.

3. Mathematical model

We have developed a steady-state mathematical model based on heat and mass transfers in each component of the unit, viz. water solar collector, air solar collector, humidifier, evaporation tower and condensation tower of

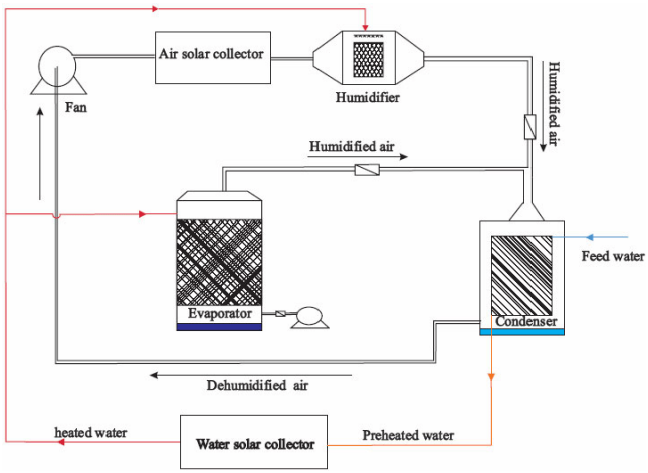

Fig. 1. Schematic diagram of the humidification–dehumidification process.

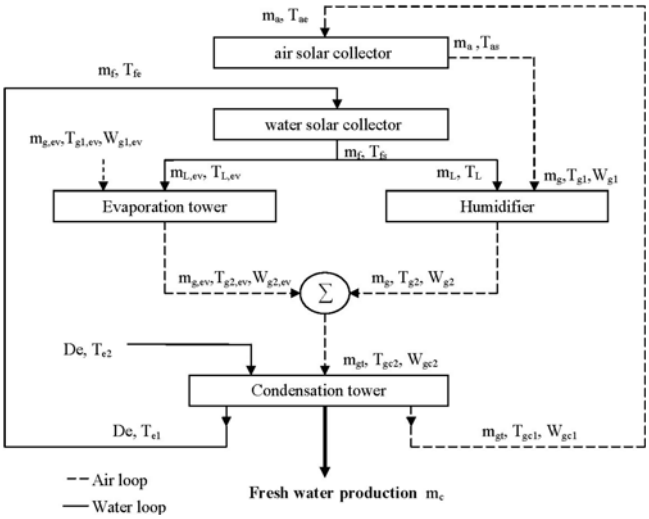

Fig. 2. Synoptic diagram of the entire process.

the desalination unit in order to numerically simulate the HD system.

3.1. Water solar collector modeling

The flat-plate water solar collector has an absorber with parallel and narrow channels. In this case, the fluid circulates in a forced convection and in one direction. The principal assumptions used to obtain the mathematical model under steady state regime are [8]:

- Speed of the fluid is uniform.
- Absorber and fluid have the same temperature at any point.
- Fluid temperature remains under 100°C point.

The energy balance equation for the system formed by the absorber and the fluid for a slice of the collector with a width of l, a length of dx and a surface of ds, is the next one:

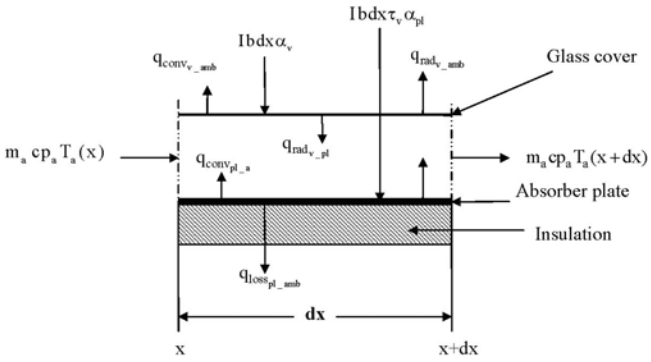

Fig. 3. Thermal energy balance of differential section of solar air collector.

$$\frac{dT_f}{dx} = \frac{U_f l}{m_f C_f}\left(\frac{BI}{U_f} + T_{amb} - T_f\right) \quad (1)$$

3.2. Air solar collector modeling

The plane air solar collector is constituted by an absorber under shape of rectangular parallel channels in copper, a glass cover and insulation. For the air solar collector, the model is based on Nafey's work [7]. The assumptions used in developing the model are listed below:

- The coefficient of exchange of the copper is very high, so we can supposes that the absorber is a flat plate.
- The velocity of air is uniform; therefore, the local state of air depends only on one side, x.
- The cross-section area of the absorber, glass cover and air are equal.
- The theoretical model employed for describing the behavior of the collector that operates in steady state is made using thermal energy balances for the three collector components—absorber plate, air and glass cover—as presented in Fig. 3.

- For the absorber plate element:

$$I\tau_v\alpha_{pl} = hrad_{pl-v}\left(T_{pl} - T_v\right) + U_{loss}\left(T_{pl} - T_{amb}\right) + hcon_{pl-a}\left(T_{pl} - T_a\right) \quad (2)$$

- For an air element:

$$\frac{dT_a}{dx} = \beta_1\left(T_{pl} - T_a\right) + \beta_2\left(T_v - T_a\right) \quad (3)$$

- For the glass cover element:

$$I\alpha_v = hrad_{v-pl}\left(T_v - T_{pl}\right) + hcon_{v-a}\left(T_v - T_a\right) + hcon_{v-amb}\left(T_v - T_{amb}\right) \quad (4)$$

3.3. Humidifier modeling

The humidifier may be represented as shown in Fig. 4. Salt water enters the system at the top of the humidifier at a temperature T_{L2} and an enthalpy H_{L2} and leaves at the bottom of the section at a temperature T_{L1} and an enthalpy H_{L2}. Air is introduced at the right side of the humidifier at a temperature T_{g1}, a humidity W_{g1} and an enthalpy H_{g1}. Air leaves at the left side of the humidifier at a temperature T_{g2}, a humidity W_{g2} and an enthalpy H_{g2}. The mass velocity of air is m_g. The mass velocities of the water at the outlet and inlet are, respectively, m_{L1} and m_{L2}.

The method of setting up the mass, thermal and enthalpy balances will be undertaken with the following simplifying assumptions:

- the process is adiabatic,
- the air and water flows are in counter-current and one-dimensional,
- the specific heat of water is constant during its passage by the humidifier,
- the equations are written as if the transfer were from air to water.

Consider a differential width, dx, across the contacting area as shown in Fig. 4, which shows the differential section of the contacting area is divided in three control volumes air, water and interface to set up the heat, mass and enthalpy balance equations.

The heat transfer equation for the air side is:

$$\frac{dT_g}{dx} = \frac{h_g a_h\left(T_i - T_g\right)}{m_g C_g} \quad (5)$$

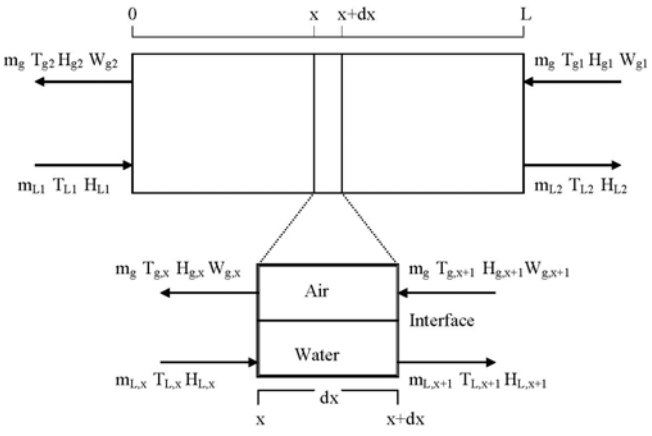

Fig. 4. Element of volume of the humidifier.

The heat transfer equation for the water side is:

$$\frac{dT_L}{dx} = \frac{h_L a_h\left(T_i - T_L\right)}{m_L C_L} \quad (6)$$

The global enthalpy equation is:

$$m_L C_L dT_L = m_g C_g dT_g + m_g \lambda_o dW_g \quad (7)$$

The mass transfer equation on the interface is:

$$\frac{dW_g}{dx} = \frac{K_m a_h\left(W_i - W_g\right)}{m_g} \quad (8)$$

To be numerically integrated, the above equations are completed with both empirical correlations of the voluminal heat coefficients ($h_l a_h$,$h_g a_h$) and the mass transfer coefficient ($K_m a_h$) that were obtained by Ben Amara et al. [9] and an algebraic equation of the curve of saturation of water steam [10].

$$h_L a_h = 25223.5 m_L^{0.0591} m_g^{0.1644} L^{-0.0542}$$

$$K_m a_h = 0.6119 m_L^{0.1002} m_g^{0.3753} L^{-0.0986}$$

The air-film voluminal heat transfer coefficient and the voluminal mass transfer on the air-water interface are related by Lewis relation [11], which is applicable for low concentration of water vapor in air provided the area of heat and mass transfer are the same, as follows:

$$h_g = C_g K_m$$

The curve of saturation of water steam is given by the following equation:

$$W_i = 0.62198 \frac{P_i}{1 - P_i}$$

3.4. Evaporation tower modeling

The principle of functioning of the evaporation tower is the same as the humidifier but the evaporation tower differs from the latter by both the geometric dimensions and the type of garnishing. The tower may be modeled as shown in Fig. 5. Air flow rates enters the bottom of the tower at a temperature $T_{g1,ev}$ and a humidity $W_{g1,ev}$. The mass velocity of air is $m_{g,ev.}$ The air flow rates exit at the top of the tower at a temperature $T_{g2,ev}$ and a humidity $W_{g2,ev}$.

Water is pulverized at the top of the tower with a temperature $T_{L2,ev}$ and no evaporated water is in the bottom of the tower with a temperature $T_{L2,ev}$. The mass velocity of water is $m_{L,ev}$.

The formulation of the mathematical model is based on Ben Bacha's work [8], and was obtained by applying the thermal and mass transfers on an element of volume of height dz as presented in Fig. 5. The mathematical model for the evaporation tower is formed by the following system of equations:

- Heat transfer equation for the water side is:

$$\frac{dT_{L,ev}}{dz}=\frac{h_L a_{ev}\left(T_{L,ev}-T_{i,ev}\right)}{m_{L,ev}C_L} \quad (9)$$

The heat transfer equation for the air side is:

$$\frac{dT_{g,ev}}{dz}=\frac{h_g a_{ev}\left(T_{i,ev}-T_{g,ev}\right)}{m_{g,ev}C_g} \quad (10)$$

The mass transfer equation for the air side is:

$$\frac{dW_{g,ev}}{dz}=\frac{K_m a_{ev}\left(W_{i,ev}-W_{g,ev}\right)}{m_{g,ev}} \quad (11)$$

The mass transfer equation on the air-water interface is:

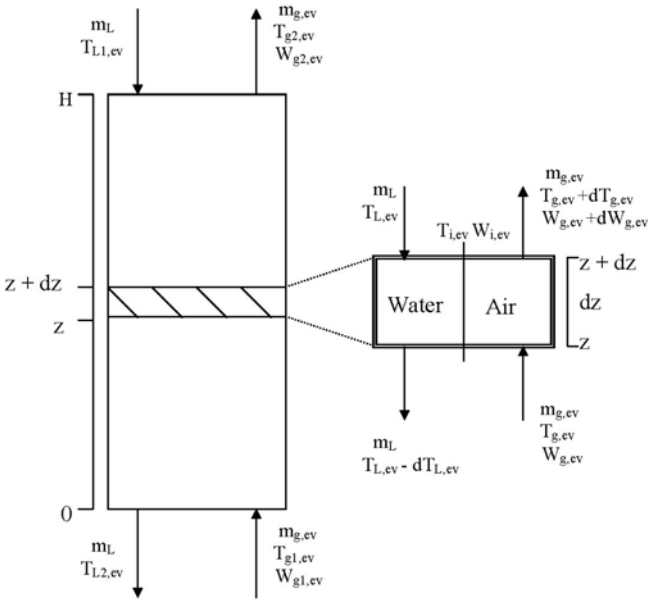

Fig. 5. Element of volume of the evaporation tower.

$$h_L a_{ev}\left(T_{L,ev}-T_{i,ev}\right)=h_g a_{ev}\left(T_{i,ev}-T_{g,ev}\right)+\lambda_o K_m a_{ev}\left(W_{i,ev}-W_{g,ev}\right) \quad (12)$$

Like the mathematical model of the humidifier, to solve the above system of equations, it is necessary to complete these equations with empirical correlations of the voluminal heat coefficients ($h_l a_{ev}$,$h_g a_{ev}$) and mass transfer coefficient ($K_m a_{ev}$) developed by Ben Bacha et al. [8] and an algebraic equation of the curve of saturation of water steam [10].

$$h_L a_{ev}=5900 m_{L,ev}^{0.169} m_{g,ev}^{0.5894}$$

$$K_m a_{ev}=2.09 m_{L,ev}^{0.45} m_{g,ev}^{0.11515}$$

The voluminal mass transfer coefficient for the air–water mixture is determined beforehand by the Lewis relation:

$$h_{g,ev}=C_{g,ev}K_{m,ev}$$

The curve of saturation of water steam is given by the following equation:

$$W_{i,ev}=0.62198\frac{P_{i,ev}}{1-P_{i,ev}}$$

3.5. Condensation tower modeling

The steady-state mathematical formulation has been developed with thermal and mass balance. This formulation gives the coupling equations between the temperature of the cooling water of the condensation tower and the humid air temperature and water content. The balances are done on an element of volume of the tower of height dz (Fig. 6). The principal assumptions used for establishing the mathematical formulation are presented in the literature by Ben Bacha et al. [8].

The respective equations for the cooling water, air mixture and air-condensate interface are written as:

$$\frac{dT_e}{dz}=\frac{UA\left(T_{ic}-T_e\right)}{D_e C_e} \quad (13)$$

$$\frac{dT_{gc}}{dz}=\frac{h_{gc}A\left(T_{gc}-T_{ie}\right)-\lambda_o K_{mc}A\left(W_{gc}-W_{ic}\right)}{m_{gt}C_{gc}} \quad (14)$$

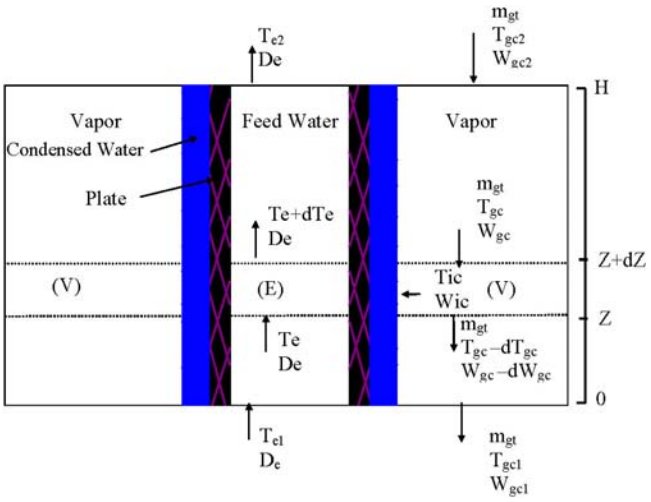

Fig. 6. Element of volume of the condensation tower.

$$\frac{dW_{gc}}{dz}=\frac{K_{mc}A\left(W_{ic}-W_{gc}\right)}{m_{gt}} \tag{15}$$

$$W_{ic}=W_{gc}+\frac{h_{gc}\left(T_{gc}-T_{ic}\right)+U\left(T_{e}-T_{ic}\right)}{\lambda_{o}K_{mc}} \tag{16}$$

The condensation rate is determined using an algebraic equation that relates the variation of the water content with the height of the tower:

$$dm_{c}=K_{mc}A\left(W_{ic}-W_{gc}\right)dz \tag{17}$$

The relationships giving the water vapor mass transfer coefficient at the air-water interface (K_{mc}), the heat transfer coefficient (h_{gc}) and the overall heat transfer coefficient (U) are presented in the Appendix.

4. Simulation, results and discussion

The set of equations presented above is used to determine the outlet parameters (air temperature, water temperature and amount of water in the air) of each components of the desalination unit with guessing the inlet of the same parameters. For this purpose, the set of ordinary differential equations is converted to a set of algebraic equations by a functional approximation technique: the orthogonal collocation. The numerical simulation allows us the understanding and the characterization of the steady-state behavior of each component of the unit. A numerical computer program is developed using the Borland C++ software to solve the mathematical models.

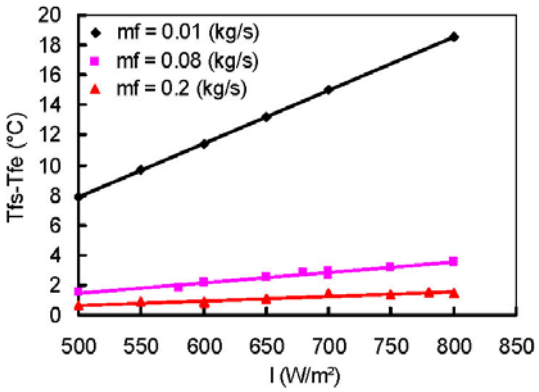

Fig. 7. Effect of solar radiation and flow rate of fluid on the temperature rise

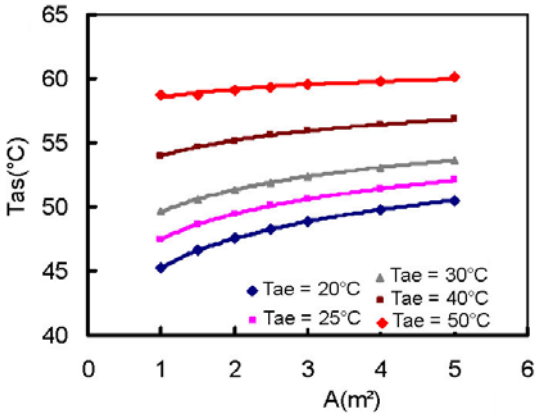

Fig. 8. Impact of both the area of air solar collector and the inlet temperature on the outlet temperature of air solar collector

The properties of each component constituting the desalination unit used in simulation are presented in Table 1.

Figs. 7 and 8 show simulation results respectively for the temperature difference of the water solar collector and the outlet air temperature of air solar collector. The temperature of fluid at the inlet of the collector depends on the ambient temperature. Therefore, we study the variation of the temperature difference according to solar radiation and fluid flow rate instead of the exit temperature.

Fig. 7 indicates that for a constant fluid flow rate, fluid temperature rise increases with increasing the solar radiation. For low values of fluid flow rate about 0.01 kg/s and for the same value of solar radiation, the temperature rise is increased more than the one for the relatively elevated flow rate such as 0.2 kg/s.

Fig. 8 illustrates the variation of the outlet air temperature, T_{as} as a function of air solar collector surface for various values of entrance temperatures, T_{ae}. The first item that can be seen from this figure is that for the high values of entrance temperatures, thereabouts 50 °C, the surface of

Table 1
Properties of each component constituting the desalination unit used in simulation

Components	Description	Value/type
Air solar collector	Aperture area, m^2	2
	Absorber plate material	Copper
	Absorptivity of plate	0.9
	Absorptivity of glass cover	0.1
	Back insulation, thickness, mm	Polyurethane, 20
	Emissivity of plate	0.94
	Emissivity of glass cover	0.987
	Transmissivity of glass cover	0.875
Water solar collector	Aperture area, m^2	2.4
	Effective transmission absorption	0.7
	Riser tube material	Copper
	Absorber surface	Pain mat black
	Loss coefficient, $W/m^2.K$	4.8
	Back insulation, thickness, mm	Fibre glass, 50
Humidifier	Size, m	0.5 × 0.5 × 0.7
	Garnishing	Cellulosic material
Evaporation tower	Size, m	0.5 × 0.5 × 1.5
	Garnishing	Thorn tree
Condensation tower	Size, m	0.5 × 0.5 × 1.5

air solar collector has an insignificant influence on the outlet temperature. The second item is that the highest outlet air temperature is obtained for the smallest values of inlet air temperatures, for instance, for a 2 m^2 of air solar collector and a value of T_{ae} equal to 25°C, T_{as} takes the value of the order of 49°C, that is to say one can have a gain of heating of the order of 96%, while for a value of T_{ae} equal to 50°C, T_{as} takes a value of the order of 59°C, which is equivalent to an increase of 18%. Therefore, according to these results, one can conclude that it is interesting to work with low temperatures at the entrance of the sensor to allow the latter to provide a better output.

The temperature of water at the entrance of the evaporation tower ($T_{L2,ev}$) can vary remarkably during the day; it ranges from 30°C in the morning to 90°C at midday. So, it is necessary to determine the influence of this parameter on the behavior of the outlet parameter. Figs. 9 and 10 show the effect of water temperature at the entrance of the evaporation tower, respectively, on air temperature and humidity at the outlet of the latter. From these figures we can note that increasing the water temperature ($T_{L2,ev}$) provokes an elevation of both the temperature ($T_{g2,ev}$) and the humidity ($W_{g2,ev}$) of humid air at the outlet of the evaporation tower. The elevation of $W_{g2,ev}$ may be confirmed by using the psychometric diagram of humid air. In fact, increasing the temperature of the moist air leads to a reduction of its relative humidity.

The impact of air and water flow rates on the humidity at the outlet of humidifier is shown in Fig. 11 in which the

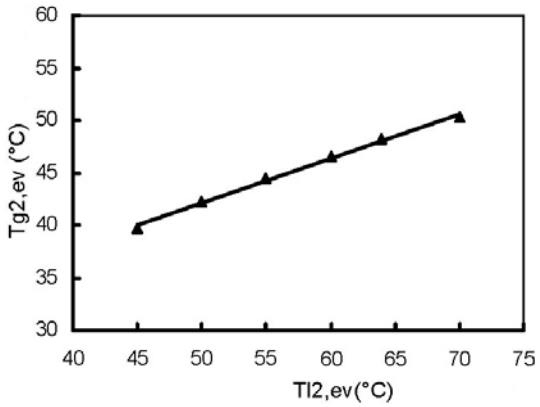

Fig. 9. Effect of water temperature at the entrance of the evaporation tower on air temperature at the outlet of the latter.

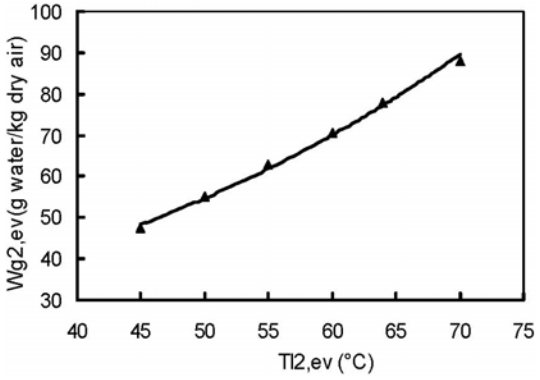

Fig. 10. Effect of water temperature at the entrance of the evaporation tower on the humidity at the outlet of the latter.

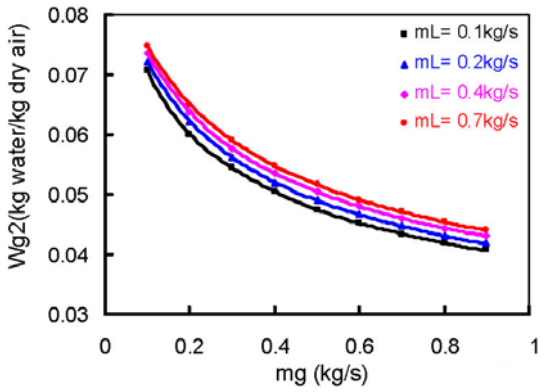

Fig. 11. Impact of air and water flow rates on the humidity at the outlet of the humidifier.

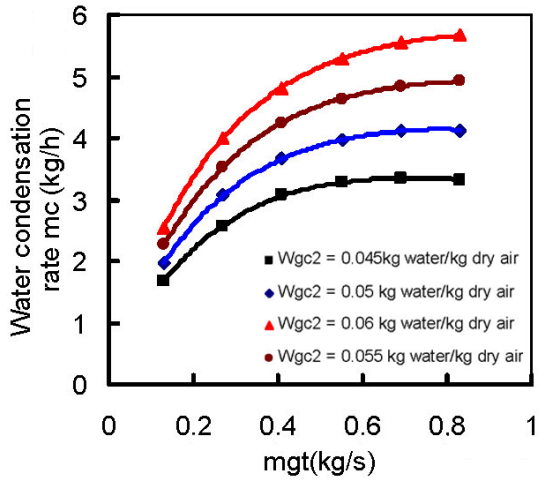

Fig. 12. Effect of air flow rate and specific humidity at the inlet of the condenser on the water condensation rate.

humidity, W_{g2} decreases with increasing the air flow rate m_g in the humidifier. This may be because the increasing of air flow rate leads to increasing the air velocity. Thus, the latter will not be charged completely with steam of water while crossing the humidifier.

Three key parameters of air are considered in the parametric study of the condensation tower. These are humidity of air at the condensation tower entrance (W_{gc2}), air flow rate (m_{gt}) and the air temperature at the entrance of the condensation tower (T_{gc2}).

Fig. 12 indicates that the water condensation rate increases meaningfully with the moist air flow rate and the inlet absolute humidity. This is due to the fact that increasing the inlet absolute humidity increases the quantity of water vapor loaded with moist air flow rate and, therefore, increases the water condensation rate.

Furthermore, increasing the moist air flow rate is followed by mass and heat transfer coefficients increase inside the condensation tower, which ultimately raises the water condensation rate. So, it is useful to work with both

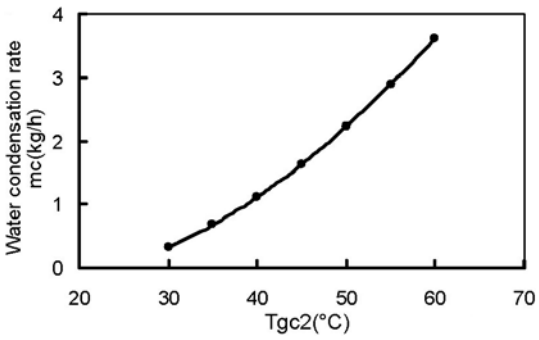

Fig. 13. Air temperature impact at the condensation tower inlet on the water condensation rate.

moist air flow rate and specific humidity high values at the condensation tower inlet.

Fig. 13 shows that the water condensation rate increases significantly and accordingly to the air temperature (T_{gc2}) at the condensation tower inlet.

5. Conclusions

This work was developed in order to ameliorate the production of the SMCEC by integrating into the latter a humidifier and an air solar collector. Therefore, the unit is composed of five components: air solar collector, water solar collector, humidifier, evaporation tower and condensation tower. A global mathematical model expressing the heat and mass transfers in each component of the unit is formulated. The developed model is simulated to study the behavior of each component of the unit as a function of meteorological and functioning conditions. The numerical simulation results presented in this paper show that:

1. The water temperature rise at the output of the solar collector increases linearly with increasing solar radiation and the highest values of the temperature rise was obtained for the smallest values of water flow rate.
2. The area of air solar collector has an insignificant effect on the air exit temperature for the high values of air entrance temperature and vice-versa.
3. The water temperature at the entrance which is at the top of the evaporation tower has a significant influence on both the exit humidity and temperature of moist air.
4. The humidity of air at the outlet of the humidifier increases with increasing the water flow rate and decreases with increasing the air flow rate.
5. The water condensation rate increases with increasing the absolute humidity at the inlet of the condensation tower, air temperature inlet and moist air flow rate.
6. The realization of this new design of the SMCEC unit is currently taking place at the National School of Engineering of Sfax, Tunisia.

To optimize the current desalination unit design, we should take into account the following recommendations:

- In order to reduce energy losses, we would rather use cylindrical evaporation tower and the condensation tower geometry than parralleliped geometry.
- A perfect insulation of each unit component would be reliable and effective.
- A good selection of the packed bed materiel provides higher exchange coefficients.
- It is advisable to integrate a storage tank to ensure a continuous use of the unit.

6. Symbols

A — Air–water exchanger area in the condensation tower, m^2
a — Air–water exchanger area, m^2
B — Effective transmission absorption product ($B = \tau\alpha$)
C_e — Water specific heat, J/(kg.K)
C_f — Fluid specific heat, J/(kg.K)
C_g — Moist air specific heat in the humidifier, J/(kg.K)
C_{gc} — Moist air specific heat in the condensation tower, J/(kg.K)
$C_{g,ev}$ — Moist air specific heat in the evaporation tower, J/(kg.K)
C_p — Air specific heat, J/(kg.K)
D_e — Water mass velocity in the condensation tower, kg/(m^2.s)
D_{h1} — Hydraulic diameter of air flow, m
D_{h2} — Hydraulic diameter of water flow, m
e — Thickness of the condenser plate, m
g — Gravitational acceleration, m/s^2
Gr — Grashof number
H_g — Enthalpy of air, J/kg
H_L — Enthalpy of water, J/kg
h — Heat transfer coefficient, J/(kg.K)
h_g — Air heat transfer coefficient at the air–water interface, W/(m^2.K)
h_L — Water heat transfer coefficient at the air–water interface, W/(m^2.K)
I — Solar flux, W/m^2
K — Thermal conductivity, W/(m K)
K_m — Water vapor mass transfer coefficient at the air–water interface, kg/(m^2.s)
m — Mass flow rate, kg/s
m_c — Water condensation rate, kg/s
m_{gt} — Total mass velocity of moist air in the condenser, kg/(m^2.s)
P_i — Saturation pressure, Pa
Pr — Prandtl number
Re — Reynolds number
q — Heat flux, W/m^2
S — Surface area of the absorber of the water solar collector, m^2
T — Temperature, K
T_i — Temperature at the air–water interface, K
U — Overall heat transfer coefficient in the condensation tower, W/(m^2.K)
U_f — Overall energy loss from the absorber to outside, W/(m^2.K)
W — Air humidity, kg water/kg dry air
W_i — Saturation humidity, kg water/kg dry air
x — Coordinate in the flow direction, m
z — Thickness, m
Z — Coordinate in the flow direction, m

Greek

α — Absorbance of the collector absorber surface
λ_o — Latent heat of water evaporation, J/kg
λ_e — Water thermal conductivity, W/m K
λ_c — Condensed water thermal conductivity, W/m K
λ_{gc} — Humid air thermal conductivity in the condensation tower, W/m K
ρ_c — Water density, kg/m^3
μ_c — Dynamic viscosity of condensed water, Ns/m^2
σ — Stefan–Boltzmann constant
ν — Velocity of fluid, m/s
τ — Transmittance

Subscripts

1 — Tower bottom
2 — Tower top
a — Air
amb — Ambient
c — Condensation tower
conv — Convection
e — Cooling water
ev — Evaporation tower
f — Fluid
g — Moist air
h — Humidifier
ins — Insulation
loss — Loss to ambient
pl — Absorber plate
rad — Radiation

References

[1] F. Ben Jemaa, I. Houcine and M.H. Chahbani, Potential of renewable energy development for water desalination in Tunisia, Renew. Ener. J., 18 (1999) 331–347.
[2] I. Houcine, F. Ben Jemaa, M.H. Chahbani and M. Maalej, Renewable energy sources for water desalting in Tunisia, Desalination, 125 (1999) 123–132.
[3] H.E.S. Fath, Desalination technology. The role of Egypt in region, IWTC, Alexandria, Egypt 2000.
[4] S. Al-Hallaj and J.R. Selman, A comprehensive study of solar desalination with a humidification dehumidification cycle, MEDRC Series of R&D reports, Project No. 98-BS-032b, 2002.

[5] J. Orfi, N. Galanis N and L. Laplante, Air humidification–dehumidification for a water desalination system using solar energy, Desalination, 203 (2007) 471–481.
[6] G. Al-Enezi, H. Ettouney and N. Fawzy, Low temperature humidification dehumidification desalination process. Energy Conv. Manage., 47 (2006) 470–484.
[7] A.S. Nafey, H.E.S. Fath, S.O. El-Helaby and A.M. Soliman, Solar desalination using humidification dehumidification processes. Part I. A numerical investigation, Energy Conv. Mgmt., 45(7–8) (2004) 1243–1261.
[8] H. Ben Bacha, M. Bouzguenda, M.S. Abid and A.Y. Maalej, Modeling and simulation of a water desalination station with solar multiple condensation evaporation cycle technique. Renew. Ener., 18 (1999) 349–365.
[9] M. Ben Amara, I. Houcine, A.A. Guizani and M. Mâalej, Theoretical and experimental study of a pad humidifier used on an operating seawater desalination process, Desalination, 168 (2004) 1–12.
[10] ASHRAE, Fundamental Handbook, Vol. 5, 1977.
[11] M.A. Younis, M.A. Fahim and N. Wakao, Heat input-response in cooling tower-zeroth moments of temperature variations. J. Chem. Eng. Japan, 20 (1987) 614–618.

Appendix

$$hcon_{pl-a} = hcon_{v-a} = 0.0336\left(\frac{K}{L}\right)\left(\frac{Lv_a}{\nu}\right)^{0.8}$$

$$hrad_{pl-v} = \frac{\sigma\left(T_{pl}^2 + T_v^2\right)\left(T_{pl} + T_v\right)}{\frac{1}{\varepsilon_{pl}} + \left(\frac{1}{\varepsilon_v} - 1\right)}$$

$$hcon_{pl-amb} = hcon_{v-amb} = 5.7 + 3.8V_{wind}$$

$$hrad_{v-amb} = \varepsilon_v \sigma\left(T_v^2 + T_{amb}^2\right)\left(T_v + T_{amb}\right)$$

$$U_{loss} = \frac{1}{\frac{1}{hcon_{pl-amb}} + \frac{z_{ins}}{K}}$$

$$U = \frac{1}{\frac{1}{he} + \frac{e}{\lambda_p} + \frac{1}{hc}}$$

$$h_{gc} = 0.479\frac{\lambda_{gc}}{D_{h1}}Gr^{1/4}$$

$$h_e = 0.023\frac{\lambda_e}{D_{h2}}\mathrm{Re}^{0.8}\mathrm{Pr}^{0.33}$$

$$h_c = \sqrt[4]{\frac{\rho_c^2 g \lambda_o \lambda_c^3}{4\mu_c z\left(T_{ic} - Tp\right)}}$$

$$K_{mc} = \frac{h_{gc}}{C_{gc}}$$

$$\beta_1 = \frac{bhcon_{pl-a}}{m_a C_a}$$

$$\beta_2 = \frac{bhcon_{v-a}}{m_a C_a}$$

$$\ln\left(P_i\right) = -6096.938\frac{1}{T_i} + 21.240964 - 2.7111910^{-2}T_i + 1.6739510^{-5}T_i^2 + 2.43350\ln\left(T_i\right)$$